

THE SPACE MOTION OF THE GLOBULAR CLUSTER NGC 6397¹

JASONJOT S. KALIRAI,^{2,3} JAY ANDERSON,⁴ HARVEY B. RICHER,⁵ IVAN R. KING,⁶ JAMES P. BREWER,⁵ GIOVANNI CARRARO,⁷
SAUL D. DAVIS,⁵ GREGORY G. FAHLMAN,⁸ BRAD M. S. HANSEN,⁹ JARROD R. HURLEY,¹⁰ SÉBASTIEN LÉPINE,¹¹
DAVID B. REITZEL,⁹ R. MICHAEL RICH,⁹ MICHAEL M. SHARA,¹¹ AND PETER B. STETSON⁸

Received 2006 September 19; accepted 2007 January 24; published 2007 February 7

ABSTRACT

As a by-product of high-precision, ultra-deep stellar photometry in the Galactic globular cluster NGC 6397 with the *Hubble Space Telescope*, we are able to measure a large population of background galaxies whose images are nearly pointlike. These provide an extragalactic reference frame of unprecedented accuracy, relative to which we measure the most accurate absolute proper motion ever determined for a globular cluster. We find $\mu_\alpha \cos \delta = 3.56 \pm 0.04$ mas yr⁻¹ and $\mu_\delta = -17.34 \pm 0.04$ mas yr⁻¹. We note that the formal statistical errors quoted for the proper motion of NGC 6397 do not include possible unavoidable sources of systematic errors, such as cluster rotation. These are very unlikely to exceed a few percent. We use this new proper motion to calculate NGC 6397's *UVW* space velocity and its orbit around the Milky Way and find that the cluster has made frequent passages through the Galactic disk.

Subject headings: astrometry — galaxies: photometry — globular clusters: individual (NGC 6397) — methods: data analysis — stars: kinematics

Online material: color figure

1. INTRODUCTION

Absolute proper motions of Galactic globular clusters are a necessity for determining the orbits of these systems around the Milky Way. These orbits are calculated by combining the proper motion of a cluster with its radial velocity and distance from the Sun and assuming a Galactic potential. The resulting space motion can constrain processes of cluster origin and destruction as well as Galactic dynamics. By studying a large set of globulars with different demographics (e.g., metallicity), cluster subsystems can be identified and used to understand formation scenarios of the various Milky Way components (e.g., Dinescu et al. 1999; Dauphole et al. 1996; Searle & Zinn 1978).

Historically, the transverse motions of Galactic globular clusters have been determined by comparing positions of their stars on photographic plates taken decades apart. The resulting observed motions are then converted to absolute proper motions by using a set of extragalactic objects to provide a zero-motion reference frame (e.g., Klemola et al. 1987), by using field stars whose absolute proper motions are known (e.g., Hanson et al. 2004), or by using secular parallaxes of field stars (e.g., Cudworth

1979). A summary of the kinematical studies of Galactic globular clusters using these different approaches is given in Dinescu et al. (1999). For many of the clusters, the proper motions have large errors, $\sim 1\text{--}2$ mas yr⁻¹, mainly because of the small number of reference objects and their low astrometric accuracy. Magnitude/color-dependent errors as well as aberrations near the edges of the photographic plates also contribute to the large errors in the absolute proper motions.

NGC 6397, one of the earliest discovered globular star clusters (de Lacaille 1755), is at $\alpha_{J2000.0} = 17^{\text{h}}40^{\text{m}}42.3^{\text{s}}$, $\delta_{J2000.0} = -53^{\circ}40'29.0''$ ($l = 338.2^{\circ}$, $b = -11.96^{\circ}$). It is the second nearest globular cluster to the Sun ($d \sim 2600$ pc; Gratton et al. 2003) and one of the most metal-poor in the Milky Way, $[\text{Fe}/\text{H}] = -2.0$ (Gratton et al. 2003). The previous wealth of data on the cluster has constrained most properties of NGC 6397, but the cluster's absolute proper motion has been measured only twice. Cudworth & Hanson (1993) report the absolute proper motion of NGC 6397 to be $\mu_\alpha \cos \delta = 3.30 \pm 0.50$ mas yr⁻¹, $\mu_\delta = -15.20 \pm 0.60$ mas yr⁻¹. The error bars in these measurements may have been underestimated; they relate to the comparison of the mean motion of field stars with the prediction from a model. The second measurement of the proper motion of NGC 6397 (Milone et al. 2006) is based on a sample of ~ 30 galaxies measured with the *Hubble Space Telescope* (*HST*) Wide Field Planetary Camera 2 (WFPC2) and appeared during the writing of this Letter. Their values are $\mu_\alpha \cos \delta = 3.39 \pm 0.15$ mas yr⁻¹ and $\mu_\delta = -17.55 \pm 0.15$ mas yr⁻¹, $\sim 15\%$ larger than the measurement reported by Cudworth & Hanson (1993) (see § 3).

In this Letter, we present a direct measurement of the proper motion of NGC 6397 relative to a large sample of galaxies, using deep photometry, astrometry, and morphological distinction between stars and galaxies.

2. THE DATA

2.1. Image Analysis

We imaged a single field of the globular star cluster NGC 6397 in 2005 March and April with the Advanced Camera for

¹ Based on observations with the NASA/ESA *Hubble Space Telescope*, obtained at the Space Telescope Science Institute, which is operated by the Association of Universities for Research in Astronomy, Inc., under NASA contract NAS5-26555. These observations are associated with proposal GO-10424.

² University of California Observatories/Lick Observatory, University of California at Santa Cruz, Santa Cruz, CA; jkalirai@ucolick.org.

³ Hubble Fellow.

⁴ Department of Physics and Astronomy, Rice University, Houston, TX.

⁵ Department of Physics and Astronomy, University of British Columbia, Vancouver, BC, Canada.

⁶ Department of Astronomy, University of Washington, Seattle, WA.

⁷ Andes Fellow, Departamento de Astronomía, Universidad de Chile, Santiago, Chile; and Department of Astronomy, Yale University, New Haven, CT.

⁸ National Research Council of Canada, Herzberg Institute of Astrophysics, Victoria, BC, Canada.

⁹ Department of Astronomy and Astrophysics, University of California at Los Angeles, Los Angeles, CA.

¹⁰ Department of Mathematics and Statistics, Monash University, Clayton, Australia.

¹¹ Department of Astrophysics, American Museum of Natural History, New York, NY.

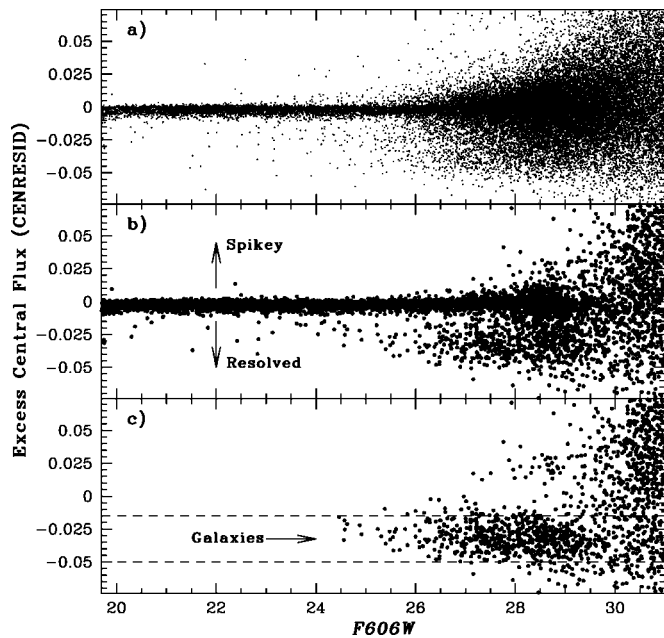


FIG. 1.—The fractional excess central flux defined by CENRESID (see § 2.1) is used to separate stars from galaxies, as discussed in § 2.3.

Surveys (ACS) on *HST* (GO-10424). The total allocated time was 126 orbits, and the observations were obtained in two broadband filters: 252 images in F814W and 126 in F606W. Several advances and refinements in data analysis were developed for the reduction of these data; these will be fully presented in J. Anderson et al. (2007, in preparation). Some details are also provided in Richer et al. (2006). Here we summarize the key steps relevant to the present Letter. We treated each local maximum in any F814W exposure as a potential detection and collated all of the peaks. We retained peaks that were found in nearly the same place in 90 images out of 252 (a 3σ detection) and were the most significant ones within 7.5 pixels. For *stellar* sources, we further required that the source meet two morphology criteria. The first, CENRESID, is defined as the fractional flux remaining within the central 3×3 pixel region of a source after the best-fitting point-spread function (PSF) has been subtracted off. The parameter is zero for stars that are well fit by the PSF. The second criteria, ELONG, measures the elongation of each source and is zero for objects that have no excess flux over the PSF fit in any direction. Finally, we eliminate false detections in the wings of bright stars and those caused by diffraction spikes. Out of the $\sim 50,000$ sources in our original catalog, 8401 *stars* survive these cuts. In addition, many extragalactic objects are found (see below).

2.2. Measuring the Proper Motions

Our *HST* ACS pointing of NGC 6397 was specifically targeted to a field $\sim 5'$ southeast of the center of NGC 6397, which had been previously studied with *HST* WFPC2 in 1994 and 1997 (King et al. 1998). The earlier observations cover about 60% of our ACS field, so that we can measure the motions of a large fraction of our objects by comparing their new positions with those at the previous epochs. We first used 3510 bright cluster stars to define a six-parameter transformation from the frame of each WFPC2 archival image into our master frame. Only cluster stars were used to define the transformations, so there is no displacement between the archival position and the

2006 position (i.e., our zero point of motion corresponds to the systemic motion of the cluster). Since a field star may happen to lie along the cluster main sequence, we iteratively rejected any star with a transformation residual >0.25 pixels in the master frame.

For each of the 50,000 detections, we used the transformations to determine where the star would be in each of the archival exposures. Since we do not a priori know the proper motion of any object that we measured on the ACS images, we examined all of the WFPC2 detections in the vicinity of the object to see which of them might correspond to the ACS detection. To compare the 1994 and 1997 archival data on the same footing, we converted each possible WFPC2 detection into an estimate for the 10 yr displacement. We then examined all of these and chose those with the same implied proper motion as successful identifications. The errors in the proper motions are calculated as the dispersion in the proper-motion measurements from the multiple first-epoch images, divided by the square root of the number of first-epoch images used.

2.3. An Extragalactic Zero-Motion Frame of Reference

The most important step in directly calculating an accurate proper motion for NGC 6397 is the choice of reference objects, which need to be extragalactic but as pointlike as possible. For this we use the morphological parameters defined earlier. The top part of Figure 1a shows the CENRESID parameter for all sources in our data, as a function of F606W magnitude. Most objects (the stars) form a tight band with CENRESID ~ 0 . In Figure 1b, we isolate those objects that pass a cut to eliminate false detections around bright stars and intersections of diffraction spikes, and for which we have measured a proper motion (see § 2.2). A clean sequence of stars is seen extending nearly to F606W = 30. A second clump of sources with negative CENRESID values is also clearly seen. Negative values imply that these objects have less flux at their centers than the PSF would predict, making them strong candidate galaxies. In Figure 1c, we isolate these galaxies by eliminating stellar objects. The dashed lines show the boundaries of our galaxy sample, $-0.05 < \text{CENRESID} < -0.015$.

This sample, selected entirely on the basis of morphology, contains 398 galaxies (one object is a clear outlier at the bright end and was therefore removed as it likely represents a field star interloper). For the best of these galaxies (bright, compact, and isolated), we can easily measure the proper motion to within 0.25 mas yr^{-1} . This is the first time that such a large sample of almost pointlike galaxies has been used to measure proper motions.

3. DERIVATION OF THE PROPER MOTION AND THE TANGENTIAL VELOCITY OF NGC 6397

To determine the proper motion of NGC 6397, we need to measure the difference in proper motion of the galaxy distribution determined above and the cluster distribution. This involves two steps. First, we convert our observed X and Y ACS pixel motions (measured relative to NGC 6397 stars) into equatorial coordinates (α , δ) by rotating the field into the correct orientation. We also multiply the motions by the pixel scale ($0''.05$) and normalize to units of milliarcseconds per year. Second, we center the mean of the 398 galaxies in the galaxy distribution to (0, 0) on this new plane with a simple translation.

Figure 2 presents our final proper-motion diagram for this field. The components are expressed in right ascension

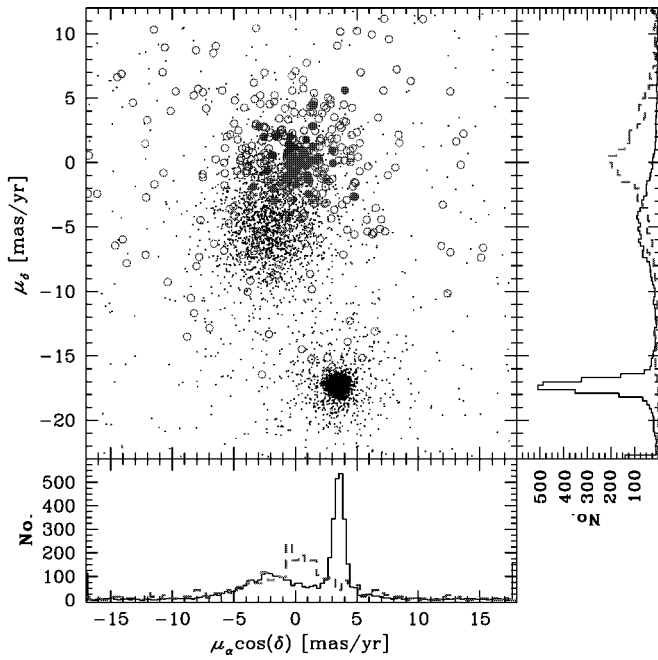


FIG. 2.—Proper-motion diagram for objects along the NGC 6397 line of sight. The tight clump near the bottom of the diagram represents cluster members, the more diffuse clump near the center of the diagram consists of field stars along the line of sight, and the larger open circles represent galaxies (see § 2.3). The 50 galaxies that provide the most weight to our measurement are shown as large filled circles. The histograms on the bottom and right better illustrate the three different populations in the proper-motion diagram. For clarity, the galaxy numbers in these two panels (*dashed curve*) have been scaled up by a factor of 7. [See the electronic edition of the *Journal* for a color version of this figure.]

and declination, such that the total proper motion $\mu = [(\mu_\alpha \cos \delta)^2 + (\mu_\delta)^2]^{1/2}$. The small dots indicate all objects that pass the criteria in § 2.1. These clearly form two clumps in the proper-motion diagram, the cluster NGC 6397 being represented with the tighter clump near the bottom of the diagram and the bulk of the field stars being concentrated in the more diffuse clump near the center of the diagram. The morphologically selected galaxies, shown as circles, also clearly clump together in this plane and have a different centroid of motion from that of the field stars. We find the centroid of the proper motions of these galaxies by taking a weighted mean, with weights $w_i = 1/(\sigma_i)^2$, where the σ_i are the estimated errors of the proper motions of the individual objects. Although the proper motions of many galaxies go into this mean, it is in fact dominated by those with the highest weight. The 50 galaxies that contribute the most to our extragalactic reference frame are distinguished as filled circles in Figure 2.

Relative to this standard of zero motion, the absolute proper motion of NGC 6397 is $\mu_\alpha \cos \delta = 3.56 \pm 0.04 \text{ mas yr}^{-1}$ and $\mu_\delta = -17.34 \pm 0.04 \text{ mas yr}^{-1}$. This is the most accurate measurement of the absolute proper motion of a globular cluster, to date. We note that our field is far removed from the cluster center, and possible cluster rotation therefore injects some additional systematic uncertainty. Given the 3.5 km s^{-1} dispersion of radial velocities (Pryor & Meylan 1993), the *maximum* observed rotational velocity is likely to be less than 2 km s^{-1} for an axial ratio of 0.93 for the cluster (White & Shawl 1987). However, we do not know what the inclination is. If we are observing the cluster pole-on, then at a point removed from the cluster center, rotation would be across the line of sight.

Considering the ellipticity, it is unlikely that this is the case. If our line of sight were perpendicular to the axis of rotation, every line of sight would have zero mean transverse velocity, because symmetry leads to a cancellation between motions in front of and behind the midpoint. Considering these effects, which are difficult to estimate, rotation might introduce an uncertainty of some modest fraction of a kilometer per second, or an amount comparable to our measuring error. Future radial velocity and proper-motion measurements over a large radial distance in the cluster may permit a derivation of this cluster rotation (see, e.g., van de Ven et al. 2006).

Our measurement of the absolute proper motion of NGC 6397 is $\sim 14\%$ larger than the Cudworth & Hanson (1993) value but is in good agreement with the recent measurement by Milone et al. (2006) within their fourfold larger error bounds. For completeness, the proper motion of NGC 6397 in Galactic coordinates is $\mu_l \cos b = -13.27 \pm 0.04 \text{ mas yr}^{-1}$ and $\mu_b = -11.71 \pm 0.04 \text{ mas yr}^{-1}$.

It is important to understand why our error is only a quarter as large as that of Milone et al. and also significantly better than other similar studies (e.g., the Kalirai et al. 2004 study of the globular cluster M4). The comparison does not reflect in any way on the quality of the measurements in these other studies, which represent the state of the art in astrometry of images of objects that look like galaxies. The difference is that we have found a method for morphological selection of a large sample of pointlike galaxies that mere eye examination cannot distinguish from stars. The best of these objects are incomparably better for astrometry than even the sharpest centered galaxies that can be recognized by eye. The measurement by Milone et al. is limited to only 33 extragalactic sources, many of which have a large dispersion and are therefore down-weighted. Their final result is derived almost entirely from a few of the brightest sources with the sharpest nuclei.

With our estimated distance of $2600 \pm 130 \text{ pc}$ to NGC 6397, we find its tangential velocity to be $v_\alpha = 43.3 \pm 2.2 \text{ km s}^{-1}$ and $v_\delta = -211.3 \pm 10.6 \text{ km s}^{-1}$. The error budget in the tangential velocity of NGC 6397 is dominated entirely by the error in the distance, which we estimate to be $\sim 5\%$. (The proper motions alone would contribute an error of $< 0.5 \text{ km s}^{-1}$.) This distance and corresponding uncertainty comes from a fit of the subdwarfs in Reid & Gizis (1998) to the new, very tightly constrained main sequence of NGC 6397 in Richer et al. (2006). The subdwarf sample has accurate parallax measurements (to within 10%), and shifting the mean distance by any more than 5% would cause a large discrepancy between these two loci that cannot be recovered by mild changes in, for example, metallicity. The third component of the cluster's motion, its radial velocity, was determined by Milone et al. (2006) to be $18.36 \pm 0.13 \text{ km s}^{-1}$.

To help interpret the velocity of NGC 6397, we now calculate the *UVW* motion of the cluster, where the *U* component is positive toward the Galactic center, *V* is positive in the direction of Galactic rotation, and *W* is positive toward the north Galactic pole (see, e.g., Johnson & Soderblom 1987). After correcting for a solar motion of $(U_\odot, V_\odot, W_\odot) = (10.00 \pm 0.36, 5.25 \pm 0.62, 7.17 \pm 0.38) \text{ km s}^{-1}$ (Dehnen & Binney 1998), we find $(U, V, W) = (-61.2 \pm 4.4, -140.5 \pm 7.0, -136.3 \pm 7.0) \text{ km s}^{-1}$. The same 5% distance uncertainty has been included in the error budget on the space motion, and again, entirely dominates the error. Relative to the Galactic center, the (Π, Θ) components of NGC 6397 are $(-46.6 \pm 4.4, 93.3 \pm 7.0) \text{ km s}^{-1}$, assuming $R_0 = 8 \text{ kpc}$ and $\Theta_0 = 225 \text{ km s}^{-1}$.

4. THE ORBIT OF NGC 6397

To integrate the Galactic orbital motion of NGC 6397, we use the initial conditions derived above and a Galactic gravitational potential with the bulge and halo represented as two spherical components and the disk represented as an axisymmetric component (see Dauphole & Colin 1995 for details). Using a Runge-Kutta fourth-order integrator with time steps of 0.1 Myr, we integrate the orbit for 5 Gyr. In Figure 3, we show NGC 6397's orbit in the disk plane (*left*) and perpendicular to the disk (*middle and right*). Clearly, the cluster's orbit is well confined within a relatively small galactocentric radius (as noted by Dauphole et al. 1996 and Milone et al. 2006). NGC 6397 orbits our Galaxy in the direction of Galactic rotation. The cluster has spent most of its time close to the Galactic disk, never reaching a height of more than ~ 3.1 kpc above the plane. The orbit crosses the plane many times, and therefore the cluster has likely experienced shocks from the Galactic disk. The timescale for this is less than 100 Myr, shorter than the half-mass relaxation time (300 Myr; Harris 1996). The apocentric radius, R_a , is found to be ~ 7.0 kpc, and therefore the cluster has not made any large excursions into the Galactic halo [eccentricity $(R_a - R_p)/(R_a + R_p) = 0.46 \pm 0.02$]. The cluster may have interacted with the Galactic bulge and suffered shocks from pericentric passages ($R_p \sim 2.6$ kpc). Given the cluster's present location ($R_{GC} = 5.7$ kpc) and velocity, we can conclude that it is approaching its apocenter.

We also tested the orbital motion assuming different starting conditions, $R_0 = 7.5\text{--}8.5$ kpc, and find that the cluster behaves very similarly to that computed above (the pericenter radii shifts by $\sim 5\%$). Although the orbit is more sensitive to the adopted distance to NGC 6397 (e.g., see Milone et al. 2006), a 5% distance uncertainty does not have a major effect on the apocenter and pericenter radii. Finally, we note that both the orbital acceleration and the perspective acceleration (caused by our line of sight intersecting a point slightly removed from the center of NGC 6397; Schlesinger 1917) of the cluster are negligible (several hundred times smaller than our error bars).

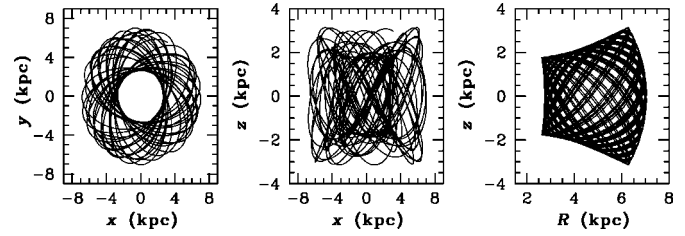


FIG. 3.—Orbit of NGC 6397 shown in the disk plane (*left*) and perpendicular to the disk (*middle and right*). The orbit shows that NGC 6397 has crossed the Galactic disk many times. The pericentric radius of the cluster orbit is found to be $R_p \sim 2.6$ kpc and the apocentric radius $R_a \sim 7.0$ kpc. Further details on the cluster orbit are provided in § 4.

5. CONCLUSIONS

The results of this Letter are a consequence of our having high-precision photometry, including morphological indices that allow the selection of starlike objects that are actually galaxies. The use of these as a reference standard has allowed us to measure the absolute proper motion of NGC 6397 with unprecedented accuracy and to compute a more reliable orbit for it. We find that the cluster has interacted with the Galactic disk and bulge many times over the past 12 Gyr. Such tidal interactions may modify the cluster mass function, and careful determination of this function coupled with dynamical models could yield evidence of this interaction (Dinescu et al. 1999).

We would like to thank A. R. Klemola, R. B. Hanson, and L. R. Bedin for discussions regarding the conversion of proper motions into space velocities and corresponding error analysis. J. S. K. is supported by NASA through Hubble Fellowship grant HF-01185.01-A, awarded by the Space Telescope Science Institute (STScI), which is operated by the Association of Universities for Research in Astronomy, Inc., under NASA contract NAS5-26555. Support for this work was also provided by grant HST-GO-10424 from NASA/STScI, the Natural Sciences and Engineering Research Council of Canada, and the Canada-US Fulbright Program.

REFERENCES

- Cudworth, K. M. 1979, *AJ*, 84, 1866
 Cudworth, K. M., & Hanson, R. B. 1993, *AJ*, 105, 168
 Dauphole, B., & Colin, J. 1995, *A&A*, 300, 117
 Dauphole, B., Geffert, M., Colin, J., Ducourant, C., Odenkirchen, M., & Tuchołke, H.-J. 1996, *A&A*, 313, 119
 Dehnen, W., & Binney, J. J. 1998, *MNRAS*, 298, 387
 de Lacaille, A. 1755, *Sur les étoiles nébuleuses du Ciel Austral* (English transl. "On the Nebulous Stars of the Southern Sky" as printed in the *Memoirs of the Royal Academy for 1755* [Paris], 194), <http://messier.obspm.fr/xtra/history/lac1755.html>
 Dinescu, D. I., Girard, T. M., & van Altena, W. F. 1999, *AJ*, 117, 1792
 Gratton, R. G., Bragaglia, A., Carretta, E., Clementini, G., Desidera, S., Grundahl, F., & Lucatello, S. 2003, *A&A*, 408, 529
 Hanson, R. B., Klemola, A. R., Jones, B. F., & Monet, D. G. 2004, *AJ*, 128, 1430
 Harris, W. E. 1996, *AJ*, 112, 1487
 Johnson, D. R. H., & Soderblom, D. R. 1987, *AJ*, 93, 864
 Kalirai, J. S., et al. 2004, *ApJ*, 601, 277
 King, I. R., Anderson, J., Cool, A. M., & Piotto, G. 1998, *ApJ*, 492, L37
 Klemola, A. R., Jones, B. F., & Hanson, R. B. 1987, *AJ*, 94, 501
 Milone, A., Villanova, S., Bedin, L. R., Piotto, G., Carraro, G., Anderson, J., King, I. R., & Zaggia, S. 2006, *A&A*, 456, 517
 Pryor, C., & Meylan, G. 1993, in *ASP Conf. Ser. 50, Structure and Dynamics of Globular Clusters*, ed. S. G. Djorgovski & G. Meylan (San Francisco: ASP), 357
 Reid, I. N., & Gizis, J. E. 1998, *AJ*, 116, 2929
 Richer, H. B., et al. 2006, *Science*, 313, 936
 Schlesinger, F. 1917, *AJ*, 30, 137
 Searle, L., & Zinn, R. 1978, *ApJ*, 225, 357
 van de Ven, G., van den Bosch, R. C. E., Verolme, E. K., & de Zeeuw, P. T. 2006, *A&A*, 445, 513
 White, R. E., & Shawl, S. J. 1987, *ApJ*, 317, 246